Carbon consequences of forest disturbance and recovery across the conterminous United States

Authors: Christopher A. Williams[1,*], G. James Collatz[2], Jeffrey Masek[2], Samuel N. Goward[3]

[1]Graduate School of Geography, Clark University, Worcester, MA, USA

[2]NASA Goddard Space Flight Center - Code 618, Biospheric Sciences Laboratory, Greenbelt, MD, USA

[3]Department of Geography, University of Maryland, College Park, MD, USA

*Corresponding Author: cwilliams@clarku.edu, P: 508-793-7323; F: 508-793-8881

Second Revision for: Global Biogeochemical Cycles

Running title: Forest disturbance and carbon dynamics

Keywords: net ecosystem productivity; carbon sequestration; forest inventory and analysis; carbon cycle modeling; forest carbon sink attribution

Abstract:

Forests of North America are thought to constitute a significant long term sink for atmospheric carbon. The United States Forest Service Forest Inventory and Analysis (FIA) program has developed a large data base of stock changes derived from consecutive estimates of growing stock volume in the US. These data reveal a large and relatively stable increase in forest carbon stocks over the last two decades or more. The mechanisms underlying this national increase in forest stocks may include recovery of forests from past disturbances, net increases in forest area, and growth enhancement driven by climate or fertilization by CO_2 and Nitrogen. Here we estimate the forest recovery component of the observed stock changes using FIA data on the age structure of US forests and carbon stocks as a function of age. The latter are used to parameterize forest disturbance and recovery processes in a carbon cycle model. We then apply resulting disturbance/recovery dynamics to landscapes and regions based on the forest age distributions. The analysis centers on 28 representative climate settings spread about forested regions of the conterminous US. We estimate carbon fluxes for each region and propagate uncertainties in calibration data through to the predicted fluxes. The largest recovery-driven carbon sinks are found in the Southcentral, Pacific Northwest, and Pacific Southwest regions, with spatially averaged net ecosystem productivity (*NEP*) of about 100 g C m^{-2} a^{-1} driven by forest age structure. Carbon sinks from recovery in the Northeast and Northern Lake States remain moderate to large owing to the legacy of historical clearing and relatively low modern disturbance rates from harvest and fire. At the continental scale, we find a conterminous U.S. forest *NEP* of only 0.16 Pg C a^{-1} from age structure in 2005, or only 0.047 Pg C a^{-1} of forest stock change after accounting for fire emissions and harvest transfers. Recent estimates of *NEP* derived from inventory stock change, harvest, and fire data show twice the *NEP* sink we derive from forest age

44 distributions. We discuss possible reasons for the discrepancies including modeling errors and
45 the possibility of climate and/or fertilization (CO_2 or N) growth enhancements.
46

1. Introduction

The global imbalance among ocean, industrial, and land use sources/sinks of CO_2 and the amount accumulating in the atmosphere implies significant net CO_2 uptake by the terrestrial biosphere [e.g. *Schimel et al*., 2001; *Tans et al*., 1990]. Despite large uncertainty about magnitude and process, analyses tend to point to northern temperate and boreal lands as dominant terrestrial sinks of CO_2 but with considerable controversy regarding attribution to specific regions or continents [e.g. *Bousquet et al*., 2000; *Fan et al*., 1998; *Gurney et al*., 2002; *Kaminski et al*., 2001; *Myneni et al*., 2001; *Tans et al*., 1990]. However, some recent work suggests far smaller sinks in northern temperate and boreal lands [*Ito et al*., 2008; *Stephens et al*., 2007; *Yang et al*., 2007].

Estimates of the conterminous U. S. forest net carbon uptake from the atmosphere range from only 10 to over 200 Tg C a^{-1} [*EPA*, 2010; *Houghton et al*., 1999; *King et al*., 2007; *Pacala et al*., 2001; *Turner et al*., 1995] in the last 2 decades. Note that here we consider the forest stock change alone rather than the forest sector stock change, where the latter also includes carbon accumulated in wood products (see State of the Carbon Cycle Report [*King et al*., 2007]).

Techniques for estimating forest carbon fluxes at regional to national scales include three approaches. The stock change method is exemplified in the US report to the United Nations Framework Convention for Climate Change [e.g. *EPA*, 2008] which uses US Forest Service Forest Inventory and Analysis (FIA) data on sequential measurement of tree diameters and/or wood volumes for about 100,000 forest plots at 5-20 year intervals. Allometric and biomass expansion factors are used to convert volume into forest carbon stocks. The rate of carbon uptake

68 is then estimated as the difference between sequential measurements divided by the number of
69 years in the interval.
70 Another technique for estimating forest carbon sinks combines estimates of the stand age
71 structure of forests with age-specific carbon accumulation rates, termed the "age-accumulation"
72 approach in this work. These carbon accumulation rates are inferred from carbon stocks as a
73 function of age [e.g. *Houghton*, 1999], known as yield tables in forestry literature, and may be
74 derived empirically from inventory estimates of stand volume and age or from a process oriented
75 dynamic growth model. Finally, forest carbon sinks have been estimated from process models
76 that account for the effects of climate variability and CO_2 and nitrogen fertilization but not
77 necessarily for land use and disturbance processes [e.g. *Schimel et al*., 2000]. These effects are
78 fully contained in the stock change method because it relies on contemporary changes in stocks,
79 but the age-accumulation approach relies on a historical characterization of carbon stock
80 accumulation and thus misses some of the contemporary influences (see Auxiliary 4).
81 Forest stock changes result from the sum of net ecosystem productivity (*NEP*), fire losses, and
82 harvest (see Figure 1). Significant decreases in harvest and fire have not been observed over the
83 past few decades so speculation as to the mechanisms underlying the stock increases have focused
84 more on growth enhancement from either climate change or fertilization with elevated carbon
85 dioxide or nitrogen [*Houghton*, 1999; *McGuire et al*., 2001; *Nemani et al*., 2002; *Pan et al*., 2009;
86 *Schimel et al*., 2000; *Zhou et al*., 2003] and on forest growth from post-disturbance recovery or
87 fire suppression [*Caspersen et al*., 2000; *Hurtt et al*., 2002; *Pacala et al*., 2001]. Though the
88 growth enhancement hypothesis has been challenged by *Casperson et al*. [2000] using forest
89 inventory data, others have argued that plausible rates of growth enhancement cannot be detected
90 using existing inventories [*Joos et al*., 2002] and recent work presents observational evidence

91 supporting a large climate change or fertilization induced sink [*Cole et al*., 2010; *McMahon et al*.,
92 2010; *Thomas et al*., 2009].

93 Disturbed forests, if not converted to another land cover type, have the potential to regrow,
94 recover, or even surpass pre-disturbance carbon stocks over decades to several hundred years.
95 The long-standing dogma of the carbon source/sink dynamics for stand-replacing disturbance
96 involves a rapid pulse emission followed by sizeable net uptake that gradually declines [*Koerner*,
97 2003; *Odum*, 1969]. This pattern is broadly supported by chronosequence observations of carbon
98 stocks [*Bond-Lamberty et al*., 2004; *Gough et al*., 2007; *Pregitzer and Euskirchen*, 2004; *Richter*
99 *et al*., 1999; *Thornton et al*., 2002] and forest-atmosphere net CO_2 exchange [*Amiro et al*., 2011;
100 *Barford et al*., 2001; *Goulden et al*., 2011; *Law et al*., 2003; *Schwalm et al*., 2007], but the precise
101 post-disturbance carbon dynamics vary by forest type and climate and this detail remains poorly
102 characterized.

103 The analysis reported here attempts comprehensive assessment of the carbon consequences of
104 past and present forest disturbance and recovery across the conterminous United States. We ask
105 if the forest age structure of the conterminous US forests accounts for the stock changes reported
106 by the FIA. Our approach utilizes the national forest inventory data (and uncertainties) to
107 constrain the forest disturbance and recovery processes represented in an ecosystem carbon cycle
108 model to obtain regional and national estimates of carbon consequences. The basic method can
109 be described as having two main steps. First, we derive forest type and climate specific post-
110 disturbance *NEP* trajectories by fitting a first-order terrestrial carbon cycle model (CASA, [*Potter*
111 *et al*., 1993; *Randerson et al*., 1996]) to grow wood stocks consistent with FIA data. Second,
112 these characteristic trajectories are applied to landscapes with forest age maps obtained from FIA
113 age distributions to derive maps of *NEP* and biomass. As such, our approach corresponds to the

114 age-accumulation method for estimating forest carbon sinks as described above. Results
115 represent carbon dynamics of forested ecoregions across the conterminous US to provide a
116 continental-scale view of forest recovery from past disturbances. In addition, we formally
117 propagate the uncertainty in FIA age-biomass trends using a Monte Carlo approach, as well as
118 examine to what degree results are sensitive to uncertainty in the model's parameterization of
119 carbon turnover time, and dependence on light, moisture, and temperature. Discrepancies
120 between FIA estimates of stock changes and those from our age-accumulation modeling are
121 assessed in terms of modeling errors and potential growth enhancements above and beyond
122 recovery, similar to *Houghton* [2003].
123

124 # 2. Methods

125 ## 2.1 Overview

126 The core of our approach is to estimate the frequency (F) of land area in a region (A_{reg}), as
127 well as the flux or stock of carbon (Q) each within strata of stand age, forest type (e.g. Aspen-
128 Birch), and site productivity (high or low) (denoted with a, f, p subscripts). Regions are defined
129 according to the Resource Planning Act Assessment by the US Forest Service. From this we
130 calculate the regional mass flux or stock ($Q_{reg,s}$) for a particular climate setting (subscript s) within
131 each region, as well as its uncertainty (δ, described further below), according to
132

133 $$Q_{reg,s} = \sum_{a} \sum_{f} \sum_{p} Q_{afp} F_{afp} A_{reg}$$

134 (1),
135

where F is the frequency of forest area adjusted to sum to unity over the three strata and obtained from the regional FIA samples of the area of forest land as described in Section 2.2, A_{reg} is the total forested area in the region, and subscripts are: a for stand age, f for forest type group, and p for productivity class. The work reported here is part of a larger project to incorporate stand age derived from Landsat time series data. In this parallel effort, specific scenes for Landsat time series were obtained from a statistically rigorous sampling procedure of forest type spatially dispersed within Eastern and Western regions [*Goward et al.*, 2008]. Here we use the climate (temperature, precipitation, incident solar radiation) and phenology for each scene (Figure 2) to simulate fluxes and stocks for each forest type and productivity class within the scene. The scenes within a region are generally good representations of the region except for the Pacific Southwest where coastal forests are not well represented. The scene level fluxes are then aggregated to regional forest fluxes and stocks by averaging across the number of climate settings (scenes, N_s) in a region as

$$Q_{reg} = \frac{1}{N_s}\sum_s Q_{reg,s}$$
$$\delta Q_{reg} = \frac{1}{N_s}\sum_s \delta Q_{reg,s} \quad (2),$$

and conterminous US estimates (subscript *nat*) are obtained from the sum over regions

$$Q_{nat} = \sum_{reg} Q_{reg}$$
$$\delta Q_{nat} = \sum_{reg} \delta Q_{reg} \quad (3).$$

156 We note that our estimates do not account for possible changes in forest carbon due to changes in
157 forest area, though in the Discussion section we explain why this is unlikely to contribute a large
158 carbon source or sink given the rates of current-day net land conversion.
159 The relationship between fluxes and stocks can be diagramed as shown in Figure 1. The so-
160 called forest sector sources/sinks refer to the net flux between the atmosphere and forest stocks
161 plus wood products stocks. The inventory approach to calculating the net forest-atmosphere flux
162 involves a measured change in carbon stocks over a specified period. A change in forest carbon
163 stocks can occur because of changes in the physiological fluxes of photosynthesis and ecosystem
164 respiration (balanced as *NEP*), as well as changes in disturbance for example by fire or harvest.
165 *NEP* can then be inferred as the difference between ΔC_{stocks} and removals from fire and harvest.
166 The net forest sector flux to the atmosphere is the sum of ΔC_{stocks} and $\Delta C_{wood\ products}$. This
167 approach, used in national reports to United Nations Framework Convention on Climate Change,
168 derives $\Delta C_{wood\ products}$ from independent harvest records and empirical decay constants for wood
169 products and landfills.
170 Our approach is to calibrate our modeled biomass as a function of age using forest inventory
171 data. We then apply the biomass and associated *NEP* from forest disturbance and recovery to the
172 landscape based on the forest area reported by the FIA within strata of age, forest types and
173 productivity classes within each region. In our modeling framework an important driver of
174 ΔC_{stocks} is net primary production (*NPP*), and the turnover times of wood and detrital pools. *NPP*
175 allocated to leaves and fine roots is quickly decomposed and cannot represent a persistent (>
176 decadal) sink. The turnover rates of wood and its immediate detrital pool, coarse woody debris,
177 are much slower, on the order of decades, and thus able to account for long-term net carbon fluxes
178 (on the order of a century). Fluxes from large stocks of slowly overturning soil pools are also

slow to respond to disturbance. By the time these large soil pools are affected by disturbance, recovery may have already occurred. This phenomenon is expressed as a low sensitivity of *NEP* to the slow turnover pools in recovering forests (see Auxiliary Material, Auxiliary 1). Of course the slow soil pools are a significant source or sink in conditions where changes in fluxes into the slow pools are large and longer term such as in permanent conversion from or to forest. This approach allows us to map *NEP* from recovery, one of the key atmospheric flux components needed to understand source/sink processes. *NEP* is a purely biological flux dependent on photosynthesis and respiration alone. Fluxes out of the forest arising from harvest or fire combine with *NEP* to produce net biome productivity (*NBP*) which is equivalent to ΔC_{stocks}. Note that we have neglected the generally smaller fluxes that contribute to *NBP* such as lateral fluxes of carbonate and organic matter in liquid form as well as volatile organic carbon emissions (see *Chapin III et al.* [2006]).

2.2 Data Sources and Modeling

Flux trajectories are derived by fitting forest growth, mortality and shedding, and allocation parameters within the Carnegie-Ames-Stanford Approach (CASA) carbon-cycle process model [*Potter et al*., 1993; *Randerson et al*., 1996] to accumulate carbon in aboveground wood biomass consistent with forest inventory data. Productivity in CASA is represented with a light use efficiency approach in which *NPP* is proportional to the fractional absorption of photosynthetically active radiation (f_{PAR}) times an efficiency term modulated by environmental conditions. *NPP* is allocated to leaves, roots, and wood which have specific turnover rates that reflect the delivery of carbon to nine detrital pools on the surface and in the soil. These pools decompose at specific turnover rates that are also modulated by environmental conditions.

202 Disturbance causes *NPP* to initially decrease, and removes or transfers carbon between live and
203 detrital pools, the atmosphere, and forest harvest. In this implementation, we adjust the default
204 rate of productivity to match carbon accumulation observed in age-accumulation trajectories from
205 forest inventory data.
206 Inventory data were obtained from the FIA field plots (FIA Database Version 4), providing
207 means and sampling errors for two attributes: 1) all live, oven-dry aboveground wood biomass,
208 and 2) area of forest land. The quotient of these attributes provides biomass per unit area. Each
209 attribute was sampled within strata of forest type group (28 classes), age (20 year age classes to
210 200+ years), and lumped into high and low productivity classes, defined as 120 to >225 cubic feet
211 $acre^{-1}$ $annum^{-1}$ and 20 to <120 cubic feet $acre^{-1}$ $annum^{-1}$ respectively. Inventory samples were
212 drawn for regions defined by the Resource Planning Act Assessment by the US Forest Service
213 that divides the conterminous U.S. into the Northeast (NE), Southeast (SE), Northern Lakes States
214 (NLS), South Central (SC), Northern Prairie States (NPS), Rocky Mountain North (RMN), Rocky
215 Mountain South (RMS), Pacific Southwest (PSW), and Pacific Northwest (PNW) region (Figure
216 2). FIA data on forest carbon and area that are available via World Wide Web download include
217 variances for each. However these variances cannot be exactly combined to estimate uncertainty
218 because of unknown covariance between carbon stock and area [*Bechtold and Patterson*, 2005].
219 Statisticians from the FIA (Charles Scott and colleagues, USFS National Inventory and
220 Monitoring Applications Center) processed the national plot data to provide our study with
221 custom products that we employed in this analysis, namely the aboveground live wood biomass
222 per unit area and its variance for each major forest type, age cohort, productivity class, for each
223 region shown in Figure 2. We confirmed that the data in this custom delivery were nearly

identical to those obtained from other web-based data servers maintained and made available by the FIA.

For this implementation we drive the CASA model with the f_{PAR} from a smoothed version of the MODIS MOD15A2 product [*Nightingale et al*., 2009] for each forest type group as well as climatological seasonality of monthly weather using NASA Goddard Institute of Space Sciences (GISS) air temperature anomalies [*Hansen et al*., 1999] added to a temperature climatology [*Leemans and Cramer*, 1991], GISS solar radiation [*Zhang et al*., 2004], and Global Precipitation Climatology Project (GPCP) precipitation [*Adler et al*., 2003]. These meteorological driver data were sampled at the 1-degree scale while f_{PAR} was provided at 1 km resolution then averaged for each forest type within each of the 28 simulation climate domains. As such, we obtain carbon flux trajectories for each combination of simulation domains (n = 28), forest-type group (n = 3 to 10), and productivity class (n = 2). Forest type group is specified at a 0.01 degree resolution obtained from *Zhu and Evans* [1994] (http://www.fia.fs.fed.us/library/maps/). Grid cell-level fractions of forest land in high and low productivity classes for each forest type and stand age within each region are specified from county level FIA data.

We modified CASA to capture disturbance impacts on the carbon cycle as follows. The post-disturbance decline and ensuing recovery of *NPP* and fractional allocation to wood (τ) are modeled as:

$$NPP(t) = NPP_{max}(1\text{-}ce^{-kt}) \quad (4),$$

$$\tau = min[1, (t - 1) / 8 \text{ years})] / 3 \quad (5),$$

where t is years since disturbance, NPP_{max} is the climatologically averaged net primary productivity independent of a disturbance legacy, c (=1.5) determines the magnitude of disturbance-induced reduction in NPP, k (=0.8) determines the rate of NPP recovery, and min is the minimum operator. We introduced this dynamic recovery of NPP after disturbance based on the well documented recovery of NPP [e.g. *Amiro et al*., 2000; *Hicke et al*., 2003]. The dynamics of allocation were intended to capture initial investment of NPP into herbaceous biomass with increasing allocation to woody vegetation with age [e.g. *Jokela et al*., 2004; *Law et al*., 2002].

In order to parameterize the amount of biomass killed by a disturbance we adopt the following treatment. Regardless of the pre-disturbance biomass, we set the post-disturbance biomass to 50% of the aboveground live wood biomass reported in the 0-20 year age class. This constrains early regrowth to pass through the youngest age-class in the FIA sample. We then estimate the corresponding fraction of live wood, leaves, and roots killed based on the ratio of their abundance prior to disturbance relative to those immediately after disturbance. Eighty percent of the disturbance-killed aboveground wood and all of the disturbance-killed leaves are assumed to be taken off site and entrained into wood products or promptly combusted and are collectively accounted for as "removals" (fire and harvest), akin to the treatment by *Turner et al*. [1995]. The remaining 20% of disturbance-killed aboveground wood is subject to on-site post-disturbance decomposition as it enters the coarse woody debris pool, also consistent with *Turner et al*. [1995]. Disturbance-killed roots decompose on-site, for which 30% of dead coarse roots are assumed to enter a belowground coarse woody debris pool, and 70% of dead coarse roots and all dead fine roots enter the soil metabolic and structural pools, broadly consistent with results presented in [*Gough et al*., 2007; *Meigs et al*., 2007]. We note that these and other prescriptions are uncertain, likely vary among disturbance and forest types, and are the subject of ongoing research. In

summary, biomass killed in a disturbance event is the difference between pre-disturbance biomass and 50% of the 0-20 year biomass reported by the FIA data. Of the killed biomass, 80% of aboveground wood and all leaves are removed (via harvest or fire) and 20% of the killed aboveground wood enters the coarse woody debris pool. The belowground wood and roots killed by disturbance remain on site to decompose. Figure 3 offers an example, in which aboveground biomass is reduced to 2.5/30 kg C m^{-2}, or <10%, and 80% of this 90% reduction in biomass is assumed to be removed (harvest or fire) while the other 20% is left to decompose on site.

With this approach it is then possible to estimate biomass removals as:

$$R = A_1 B_{pre}\left(1 - f_{left}\right) \quad (6),$$

where A_1 is the area of forested land assigned a stand age of one year based on the FIA age histogram, B_{pre} is the pre-disturbance aboveground biomass, and f_{left} (=0.8) is the fraction of biomass left to decompose on-site. Each of these varies by forest type, region, and productivity class. This estimate is subject to errors in the area of forest assigned to this young age class, the age of forests prior to disturbance and correspondingly the biomass pre-disturbance, and uncertainty in the fraction of biomass in disturbed forests that is taken off-site as wood products. Removals from non-stand replacing harvests are not considered in this approach but later in the Discussion section we attempt to quantify the impacts of this assumption.

The next step in our model parameterization involves calculating the wood production – wood age pair that allows the best match to the inventory data of aboveground stock recovery, with the following multi-step procedure. First, we calculate a target aboveground live wood biomass (B^*, in g C m^{-2}) from the mean in the 100 to 200 year old age classes, including successively younger age classes in 20 year increments to ensure a minimum of two samples. The target age (A^*, in years) is obtained from the average of old classes sampled to derive B^*. Second, we approximate

293 the rate of annual aboveground live wood biomass production (P_w, in g C m^{-2} a^{-1}), which is a
294 function of *NPP* and wood allocation, that would be required to obtain B^* by A^* for a range of
295 possible wood turnover times (A_w) spanning 30 to 300 years in increments of 10 years by solving
296 a simplified integral form of the differential equation for biomass with time ($dB/dt = P_w - B/A_w$) to
297 yield:
298
299 $$P_w = \frac{B^*}{A_w(1 - e^{\frac{-A^*}{A_w}})} \quad (7).$$
300
301 Thus, we obtain an array of possible P_w-A_w pairs that would grow the target biomass by the target
302 age. In a few particular cases this approach yielded implausible wood ages, but with negligible
303 consequence for the scales of analyses presented in this study. The third step is to select the pair
304 that provides a biomass recovery curve most like the inventory sample assessed as that which
305 minimizes the sum of squared error between modeled and sampled aboveground live wood
306 biomass. Modeled biomass is calculated at the sample ages (t, in years) according to:
307
308 $$B(t, A_w) = B_o e^{\frac{-t}{A_w}} + P_w A_w (1 - e^{\frac{-A^*}{A_w}}) \quad (8),$$
309
310 where B_0 is an assumed initial biomass of 200 g C m^{-2}. Lastly, we linearly rescale the model's
311 default monthly *NPP* values to provide an annual total NPP_{max} inferred from the fitted rate of P_w,
312 as:
313 $$NPP_{max} = \frac{P_w}{\tau\alpha} \quad (9),$$

where τ (=1/3) is the allocation of *NPP* to wood and α (=0.75) is the fraction of this that is allocated to the aboveground wood pool (stems and branches) instead of belowground (coarse roots).

Following determination of P_w and A_w parameters, characteristic carbon flux trajectories (Q_{afp}) are developed from, first, a 1000 year spin-up to steady-state carbon pools. This is followed by a disturbance prior to the disturbance of interest with 75 years of regrowth for all forest types except loblolly pine and longleaf / slash pine (30 years) and Douglas-fir (200 years). The age of trees at harvest is set to be just older than the typical peak in age histograms reported by the FIA (see Auxiliary 2, Figure A2.3), except where harvest rotations are known to be short (SE and SC pines), or where harvest over previous decades tended to target old growth forests with high economic value (Douglas-fir [*Cohen et al*., 2002]). This 'pre-disturbance' is important in that it establishes the amount of live carbon subject to disturbance-induced disposition, meaning taken off-site as removals or decomposing on-site. Finally, we simulate the most recent disturbance after which we allow 200 years of regrowth to characterize carbon dynamics with stand development. These procedures result in a group of carbon stock age trajectories analogous to yield tables.

We have not modified CASA's default treatment of heterotrophic respiration emerging from microbial decomposition of soil and litter carbon and associated transfers among carbon pools. The general equation for the rate of heterotropic respiration from a specific carbon pool is:

$$Rh_{pool} = C_{pool} k_{pool} W_{resp} T_{resp} M \,, \qquad (10),$$

where C_{pool} is the amount of carbon in a pool, k_{pool} is the pool-specific decay rate constant, W_{resp} and T_{resp} control how respiration depends on soil moisture and temperature states, and M is the carbon assimilation efficiency of the microbes. Total heterotrophic respiration is the sum of that from each of the nine detrital pools.

2.3 Uncertainty Analysis

A formal propagation of uncertainty from sampling errors (coefficient of variation, CV) for forested area (±10 to 100%) and total aboveground live biomass (±10 to 100%), and volume to carbon conversion (±7%) are all included. The uncertainty in inventory aboveground live biomass per unit area is propagated to the predicted fluxes and aboveground live biomass with a Monte Carlo procedure analogous to Tier 2 uncertainty estimation in the IPCC Good Practice Guide [*IPCC*, 2000]. The model was fit to 25 different biomass regrowth trajectories, where each trajectory was generated from random samples of the normally distributed aboveground live wood biomass for each age class (25 draws of biomass per unit area from each of 10, 20-year age classes). Forcing the fitted trajectory to conform to the assumption that biomass increases monotonically and saturates with age strongly constrains the resultant age-accumulation curves and their variances (Figure 3). An additional 7% uncertainty is used to account for tree volume to carbon conversion [*Smith and Heath*, 2001]. Put together this method involved over 130,000 simulations of age-dependent dynamics of forest carbon fluxes and stocks. The uncertainty of forest area and aboveground live biomass per unit area is obtained from the FIA data.

As shown in Equations 1-3 above, independent uncertainties in the product of flux or stock with area are combined as $\delta Q_{total} = \left(\frac{\delta Q_{afp}^{\ 2}}{Q_{afp}^{\ 2}} + \frac{\delta A_{afp}^{\ 2}}{A_{afp}^{\ 2}} \right)^{1/2}$ [*Taylor*, 1997]. We adopt a conservative assumption of non-random error propagation for which uncertainty is additive over forest types,

productivity classes, and ages, and also additive spatially for a simulation domain, a region, or the nation. This uncertainty aggregation is analogous to a Tier 1 uncertainty described in the IPCC Good Practice Guidance [*IPCC*, 2000].

Uncertainty in *NEP* also derives from model structure (not analyzed) as well as model parameterization of light, moisture, and temperature sensitivity of heterotrophic respiration and/or *NPP* expressed in the CASA model. As described in Auxiliary Material, Auxiliary 1 Section 1, we analyzed *NEP* responses to a 2% increase of six representative parameters including the maximum light use efficiency, moisture dependence of *NPP*, optimal temperature for *NPP*, turnover time of the slow soil carbon pool, and both the Q10 and moisture dependence of heterotrophic decomposition of soil carbon. We use a 2% change in parameter value in order to obtain a detectable response in *NEP* but for ease of discussion the sensitivities are divided by two and expressed as % change in *NEP* for a 1% change in parameter value (see Auxiliary Material, Auxiliary 1).

3. Results

3.1 Carbon Trajectories

Using CASA as a controlled growth model accurately reproduces the accumulation of aboveground forest carbon stocks with time since a stand replacing disturbance as informed by FIA data (Figure 3), imposing a powerful, albeit partial, observational constraint on net ecosystem carbon flux trajectories with stand age. Additional data on litter, woody debris and soil carbon dynamics would provide much needed additional constraints on estimated ecosystem C dynamics. More rapid regrowth of aboveground stocks in the high productivity class causes higher amplitude trajectories for carbon stocks and fluxes (Figure A2.1, A2.2, Auxiliary 2) with larger

post-disturbance sources that give way to stronger sinks with ensuing forest regrowth. The Monte Carlo simulation approach provides an envelope of trajectories (Figure 3) that enables formal uncertainty propagation through all scales of the analysis (regional forest types to conterminous U.S. forestlands). Absolute uncertainty surrounding *NEP* tends to peak where forest uptake is maximum (peak *NEP*) and then diminishes with forest age (Figure 3). An important exception, not shown in Figure 3, is the often large uncertainty in carbon emission in the years immediately following disturbance; large because of variation in the pre-disturbance carbon stocks and the amount of dead wood that decomposes on-site. The timing of *NEP* crossover from source to sink is surprisingly insensitive to variability in biomass accumulation (not shown), and generally occurs at ages <20 years (e.g. Figure 3 and Figure A2.1, A2.2, Auxiliary 2) consistent with many reported chronosequence fluxes [e.g. *Bond-Lamberty et al*., 2004; *Gough et al*., 2007; *Goulden et al*., 2011; *Law et al*., 2004; *Litvak et al*., 2003; *Noormets et al*., 2007; *Pregitzer and Euskirchen*, 2004]. Patterns of post-disturbance uptake of carbon in regrowing forests vary widely across regions of the conterminous U.S. as well as by forest type group and productivity class (Figure A2.1, A2.2, Auxiliary 2). Forest inventory data describing the recovery of aboveground live wood biomass carbon with stand development act as a strong constraint on the modeled carbon cycle including the rates of litter and soil carbon turnover and decay.

Our analysis of the sensitivity of the model to parameters revealed that nearly all of the sensitivities are less than 1% indicating general dampening of parameter perturbations and suggesting that uncertainties in these parameterizations do not expand as they propagate through to modeled *NEP* (see Auxiliary 1, Table A1.1). Model structure and parameter uncertainties are not included in our analysis but are expected to add about ±10% based partly on a sensitivity analysis presented in Auxiliary Material 1.

405

406 **3.2 Continental Patterns**

407 Regional variations in disturbance rates and *NEP* across the conterminous U.S. reflect
408 harvesting practices and regional climates (Tables 1 and Table A2.1, Figures A2.1, A2.2, A2.3).
409 Forests growing in relatively dry settings (e.g. Rocky Mountain South (RMS)) have low *NEP*,
410 contrasted by high carbon sequestration rates in the Pacific Southwest and Northwest, as well as
411 Southeastern and South Central regions (Table A2.1). The largest rates of disturbance, and the
412 largest sinks of carbon stimulated by forest recovery from recent disturbance ("regrowth sinks"),
413 are in Southeastern (SE), South Central (SC), and Pacific Northwest (PNW) regions. These
414 regional biologically driven sinks do not reflect net biome productivity because recovery
415 trajectories do not include the fate of disturbance-induced carbon removals such as carbon taken
416 offsite to lumber, pulp and paper mills or released promptly on-site by natural and anthropogenic
417 fires (see schematic in Figure 1). This is addressed further in the discussion where we present the
418 forest-to-atmosphere carbon exchange.

419 At the continental scale, the biological recovery sink (*NEP*) is estimated to be 164±28 Tg C a^{-1}
420 (Table 1), or about 71 g C m^{-2} a^{-1} averaged for the 230 million hectares of forestland represented
421 here. Nearly all (84%) of this *NEP* sink results from net growth of live carbon stocks with only a
422 small fraction shared among soil carbon (6%), litter carbon (2%), and coarse woody debris (8%)
423 stocks (Table 2). Our sample includes 93% of the conterminous U.S. forestland, reported to be
424 250 million hectares [*EPA*, 2008]. Our analysis did not include the Northern Prairie States region
425 (~6% of total area and ~5% of total carbon) because the effort was originally connected to a
426 Landsat remote sensing analysis whose random sample did not draw Landsat scenes for this
427 region. As verification, our stand-age histograms by region generally correspond well with a

similar presentation of the same basic data as recently published by *Pan et al*. [2011]. Comparing to regional statistics of forest area and live biomass reported in *EPA* [2008] we find good correspondence overall (Table 1).

The estimated uncertainty arising from forest area, aboveground wood biomass, and conversion of diameter measurements to volume and carbon produced relatively small uncertainty estimates in our biomass and fluxes. This is partly due to the continuous, monotonically increasing, and saturating growth form imposed by the process-model approach. This functional form is more plausible than one that would allow abrupt increases and decreases in aboveground live wood biomass with stand development (i.e. stand age) as are commonly found in the inventory data when arrayed as a chronosequence (e.g. Figure 3, 110- 150 year biomass). Imposing the model's growth form has the effect of filtering out some of the variance inherent in chronosequence trajectories of biomass with stand age. Other uncertainties arising from model structure and assumptions about disturbance severity/type, age, partial cutting, natural wood turnover, and a possible age-related decline in productivity are evaluated by judging the impacts of these factors on model output through sensitivity analyses (see Auxiliary 1, Section 2).

We used the 1km forest type map to produce a gridded map of *NEP* and its uncertainty (from variances in FIA data) for the conterminous US (Figure 4). Within each region each forest type considered was assigned the regional estimate of *NEP* for that forest type and region. Regional forest *NEP* sinks range from >25 to 200 g C m^{-2} a^{-1} with eastern and western forests generally ranging from 75 to 100 g C m^{-2} a^{-1}. The RMS region is predicted to be uniformly <50 g C m^{-2} a^{-1}. The discontinuities conforming to state borders between West Virginia and Virginia and between Washington and Idaho occur because the same forest types in each neighboring region have regionally specific and different growth and disturbance rates.

As an independent evaluation of our predicted stocks and fluxes we compared our results with five available studies on chronosequences for forest types in the conterminous US. These studies sometimes do not include estimates of both fluxes and stocks for different aged forests and estimates used various biometric and flux measurement approaches. The small number of sites with available data, variability in the data, and issues of extrapolating fine scale measurements to regional responses do not justify quantitative comparisons and demonstrate the need for more of these types of measurements and for finer scale modeling. The results of these comparisons are shown in Auxiliary 3, Figure A3.1. Agreement varies widely between the comparisons at the different sites/regions.

4. Discussion

Comparing estimates of the conterminous U.S. forest *NEP* sink from multiple studies (Table 3) reveals a general separation between age-accumulation and stock-change methods. This comparison spans estimates for the 1980s to more recent years (e.g. 2005-2006), but this may be justified because atmospheric inversions seem to indicate a long term mean sink in North America during the '80's and '90's but with large interannual variability [*Baker et al*., 2006]. Four of the six age dependent analyses that seek to represent carbon emissions and sequestration with post-disturbance recovery provide lower estimates of the forest *NEP* sink when compared to the four stock-change analyses, with 82 g C m^{-2} a^{-1} versus 154 g C m^{-2} a^{-1} averaged across their respective studies, or 189 Tg C a^{-1} versus 354 Tg C a^{-1} when integrated across US forest area. This is even true when process-oriented studies rely on forest inventory data to prescribe the rate of aboveground carbon stock recovery with time, as well as the area of forest of different ages.

For example, regarding *NEP* alone we find general agreement with *Turner et al*. [1995] who reported 203 Tg C a^{-1} compared to our estimate of 164 Tg C a^{-1}. In contrast, the *EPA* [2008] stock-change estimate of forest *NEP* is twice as large as this study's age-accumulation result (335 compared to 164 Tg C a^{-1}, Table 2). The disparity between the stock-change method and these other, age-accumulation results is likely due to large annual to decadal increases in stocks measured in the inventory that then implies greater *NEP* (regrowth). What causes this general disagreement remains unclear, though growth enhancement is a plausible explanation of the difference, consistent with recent publications [*Cole et al*., 2010; *Luyssaert et al*., 2010; *McMahon et al*., 2010; *Thomas et al*., 2009]. Effects of growth enhancement are implicit in the stock-change method but not well incorporated in the age-accumulation methods that emphasize effects of regrowth dynamics, even when these methods rely on inventory-derived chronosequences to constrain biomass accumulation as in the present study (see Auxiliary 4 for an illustration of this). There is also one study reported in Table 3 including only the effects of climate and CO_2 fertilization based on an ensemble of models for the conterminous US [*Schimel et al*., 2000]. If this sink were added to the forest recovery (age-yield table) estimates the results would be more in line with the stock change approach.

We note that the *EPA* [2008] estimate of total removals is 38% higher than that estimated with our modeling approach (=162/117, Table 3). About half of the difference is due to elevated fire emissions reported in *EPA* [2008], however this estimate is much higher than the rate of forest fire emissions being reported elsewhere (e.g. *van der Werf et al.*[2010]). This difference translates directly into the *NEP* estimated from the stock change method, and elevates the *EPA* [2008] estimate by 20 TgC a^{-1} relative to the estimate from our approach. The *EPA* [2008] report also estimates 25 TgC a^{-1} greater removals by harvest. There are two ways we could adjust our

496 methodology to try to match this rate of removal. We could either, a) increase the amount of
497 biomass removed by disturbances on average by increasing the age and hence biomass of
498 disturbed forests, b) increase the amount of biomass removed on average by removing a larger
499 fraction of pre-disturbance biomass and leaving less to decompose on site, or c) increase the area
500 of forests disturbed by increasing the young-aged fraction of forests if we believe the stand age
501 attribute offers a biased representation. All of these would increase removals but they would have
502 different effects on *NEP*. The first option would decrease *NEP* because more disturbance-killed
503 material would be left on-site to decompose and be emitted from forests. The second approach
504 would increase *NEP* because of reduced on-site decomposition. The third approach would
505 decrease *NEP* because a larger fraction of forested area would be concentrated at young stand
506 ages (<15 year old) where *NEP* is either a large negative value or near zero (Figures A2.1, A2.2).
507 And in the extreme case that we simply adjusted our *NEP* estimate upwards to cover the
508 difference in removals, the *EPA* [2008] estimate would still be 126 TgC a^{-1} higher than the
509 estimate emerging from our age-accumulation method.
510 A term-by-term comparison between stock changes reported from inventory methods and
511 those derived in the current study's age-accumulation approach indicates that a change in live
512 carbon stocks makes up a large portion of the difference in *NEP* estimated with the two methods
513 (Table 2). Annual increases in soil carbon, coarse woody debris, and litter pools are also
514 noticeably lower in the present analysis compared to those reported by the *EPA* [2008; 2010]
515 (Table 3). Because our method, necessarily, produces aboveground live wood biomass and forest
516 area estimates that are consistent with, or wholly derived from, the inventory itself (Table 1), our
517 relatively low estimate of annual changes in live stocks (Table 2) does not appear to be caused by
518 underestimation of a) stocks, or b) forest area. These differences translate to the full forest sector-

519 atmosphere net exchange, whereby the stock-change method estimates a much larger forest sector
520 C sink than obtained with this study's age-accumulation approach (Table 2).
521 Our maps of conterminous US forest *NEP* and its uncertainty (Figure 4) are one of the first of
522 which we are aware (though see *Woodbury et al*. [2007]) and will be used in further study of the
523 impact of the forest disturbance fluxes on atmospheric CO_2 as a boundary flux for atmospheric
524 transport models much as gridded fire, fossil fuel burning, and ocean CO_2 fluxes are prescribed in
525 forward and inverse atmospheric modeling [e.g. *Peters et al*., 2007]. Complete accounting of
526 forest sector fluxes would additionally require maps of fire [e.g. *van der Werf et al*., 2010] and
527 wood products emissions. These studies will allow assessment of the detection limits for the
528 magnitude and spatial variability of sinks in top-down studies.
529 This study's approach imposed a number of simplifying assumptions that were necessary
530 given the initial scope of our work. Below we address some of these and their potential
531 implications regarding interpretation of our results.
532 • We assume characteristic regrowth trajectories regardless of disturbance type even though
533 the nature of post-disturbance carbon dynamics is sure to vary between fire, harvest,
534 hurricane, and the severity of disturbance. For instance, around twice as much coarse
535 woody debris (CWD) may remain on site after a severe fire compared to clear-cut harvest
536 [*Tinker and Knight*, 2000]. This remaining detritus provides a source of CO_2 for a
537 prolonged period after disturbance. Using data reported by *Smith et al*. [2009] and the
538 National Interagency Fire Center (to account for Alaskan fires) we estimate that for the year
539 2004 the ratio of burned area to harvested area in the eastern US was about 0.30 compared
540 to 0.46 in the west. In terms of carbon removals though, our forest fire estimates from the
541 Global Fire Emissions Database v3 (10 Tg C a^{-1}) are much smaller than our estimated

harvest removals (107 Tg C a^{-1}). Because the total removals are dominated by harvest, as is the total area disturbed, accounting for differences caused by fire versus harvest would not significantly change our results or conclusions. Furthermore, some but not all of this variation is captured by the Monte Carlo approach, as well as with stratification by site productivity and across regions. Partial disturbances such as defoliation events are not represented with the current methodology, and discussed further below.

- Our assumption of equivalence between forest age and time since disturbance does not account for the effects of partial disturbance that allows older aged trees to remain among regenerating cohorts or the dynamic state of old forests that have reached the age of natural mortality and reestablishment. This particular issue has been examined by *Bradford et al.* [2008] for a subalpine forest system. In that study a large part of the age versus years since disturbance discrepancy arose in stands undisturbed for long periods of time (>200 years), longer than what we analyze in this work. From FIA data we estimate that about 3% of forested land is >200 years old for conterminous US.
- Our analysis is sensitive to biases in the ages associated with the aboveground live wood biomass trajectories, as explored in an extensive sensitivity analysis described in Auxiliary 1, Section 2. For instance, if the FIA ages are older (younger) than actual stand ages, our predicted recovery sink is underestimated (overestimated). This, of course, is an issue with any approach proposing to use FIA age structure information to estimate fluxes and stocks [e.g. *Pan et al.*, 2011]. Despite this sensitivity, we note that bias in stand age is not likely to be large enough to explain the major differences between the stock-change and age-accumulation methods (Table A1.2).

564 • The FIA data we used to construct aboveground live wood biomass trajectories include the
565 effects of partial cuts, which are a significant component of disturbance in US forests
566 contributing >50% of the total harvested area [*Smith et al.*, 2009]. Reported stand ages
567 reflect the trees not cut while the plot level biomass will be lower in these cases producing
568 lower regional aboveground live wood biomass for mid and older aged stands. These partial
569 cutting practices (e.g. salvage logging, selective logging, thinning), which remove biomass
570 from forested plots without resetting the FIA-recorded stand age, could have a substantial
571 influence on the forest *NEP* estimate. The implicit inclusion of plots that experienced
572 partial cutting (not fully stocked) likely results in correct biomass estimates but lowers the
573 slope of regrowth trajectories resulting in some underestimation of *NEP*. In an extensive
574 sensitivity analysis (Auxiliary 1, Section 2) we find strong sensitivity to such biases, with a
575 10% elevation of biomass leading to a 14% elevation of conterminous US forest *NEP*. This
576 is equivalent to a 2.3 Tg C a^{-1} increase in *NEP* for each 1% increase in biomass. Despite
577 this large sensitivity to biomass trajectories, to account for the approximately 160 Tg C a^{-1}
578 difference, the reported biomass would need to have been underestimated by 70% (=160 Tg
579 C a^{-1} / 2.3 Tg C a^{-1} per 1% increase in biomass). Additional sensitivity analyses examining
580 effects of natural, partial disturbances that lead to wood turnover and on site decomposition
581 (e.g. ice storms, blowdowns, insect damage) indicate that they are also unlikely to present a
582 large error/bias in our estimate.
583 • We do not take into account annual changes in forest area which could contribute to the
584 discrepancy between recovery and stock change approaches. The *EPA* [2008] reports
585 indicate that forest area has been increasing at a rate of 0.24% a^{-1} since 1990. If we assume
586 that new forests would range between 1 to 5 kg C m^{-2} over an age range of 0 to 20 years

587 (e.g. see Figure 3) then the average accumulation rate for these forest would be about 250 g
588 C m^{-2} a^{-1}. Correcting this for the increase in forest area produces an added 1.7 Tg C a^{-1} sink,
589 indistinguishable within the uncertainties of our method.
590 • It has been proposed that forest carbon sinks may be driven by long term trends in
591 temperature, precipitation, nitrogen deposition, and atmospheric CO_2. Responses to these
592 trends are embedded in the biomass-age trajectories from the inventories in complex ways
593 and more recent increases in growth may not be accounted for in our approach (see
594 Auxiliary 4 for a thorough examination of this). Others have addressed this and concluded
595 that forests are not responding in a systematic way to these trends [*Caspersen et al.*, 2000],
596 that forest inventory data are not precise enough to resolve expected responses to trends
597 [*Joos et al.*, 2002], and that a smaller number of inventory measurements on forests of
598 known disturbance history do indeed show strong trends in growth enhancement correlated
599 with trends in temperature and atmospheric CO_2 [*McMahon et al.*, 2010; *Thomas et al.*,
600 2009]. In a study of global terrestrial carbon sinks using CASA, *Thompson et al.* [1996]
601 showed that in order to obtain a terrestrial carbon sink of ~2 Pg C/yr broadly consistent with
602 top-down sink estimates, *NPP* has to undergo a sustained increase of 0.18% per annum.
603 Similar estimates have been reported by others [e.g. *Joos et al.*, 2002]. Our own sensitivity
604 analysis (not shown) showed that a sustained increase in *NPP* of 0.2% per annum would
605 increase live biomass in a typical 60 year old forest by approximately 5% and is thus a weak
606 or undetectable signal in a biomass chronosequence. A 0.2% annual increase in *NPP* is
607 implausibly large sensitivity of photosynthesis to CO_2 ($dNPP/NPP$ x CO_2/dCO_2 of ~0.96, or
608 near proportional response) and would require other positive feedback mechanisms such as
609 nitrogen fertilization and/or climate trends to operate in parallel. We conclude that plausible

responses of forest sinks to climate and CO_2 or N cannot be resolved with FIA biomass-age trajectories alone such as those we utilize here and that have been proposed by others [e.g. *Pan et al.*, 2011].

The approach described here is also sensitive to uncertain parameters including rates of wood mortality and coarse woody debris decomposition, as well as the amount of dead aboveground and belowground biomass left to decompose onsite following disturbance. It lacks a standing dead wood pool that may be important because it decomposes much more slowly than dead wood in contact with the forest floor [e.g. *Harmon and Hua*, 1991; *Harmon et al*., 2004; *Janisch et al*., 2005]. In our ongoing efforts, literature is being exhaustively explored to better constrain these and other parameters and processes. Additional effort is being invested in attributing disturbances to particular drivers based on spatial and geospatial records of fire and insect outbreaks. While valuable, it is unlikely that such refinements and constraints will reconcile the large differences between the age-accumulation and stock-change approaches, something that may benefit from a close collaboration with inventory experts to clarify differences of approach and accounting, as well as more comprehensive assessment of possible growth enhancement effects. Future efforts at improving this study's approach will include more detailed prescriptions of type and severity of disturbances, further comparisons with site observations as they become available, and analyses of top-down atmospheric constraints on source/sink magnitude and distributions. Estimates would also be better constrained if additional data on litter, dead wood and soil organic carbon dynamics were available from field studies.

5. Conclusions

Forest Inventory and Analysis data provide unique and valuable information about disturbance history and associated carbon stocks and fluxes with forest recovery. By using these

633 data to constrain forest growth rates in a carbon cycle model, this study provides a more detailed
634 estimate of carbon sources and sinks from recent forest disturbance and recovery across regions
635 and forest types of the US. One of our key findings is a much smaller net sink of carbon in
636 conterminous US forests than previously estimated with the stock-change approach as used in
637 UNFCCC reporting [*EPA*, 2008]. The source of across study inconsistencies among national
638 estimates of stocks and fluxes remains largely unexplained. The paucity of observed net
639 ecosystem productivity and biomass chronosequences limits our ability to evaluate modeled
640 responses. These types of observations are critically needed in order to adequately test models
641 representing disturbance and subsequent recovery.
642
643 **Acknowledgements:** We thank Charles (Chip) Scott and his team at the USFS National
644 Inventory and Monitoring Applications Center for providing us with FIA data. We acknowledge
645 helpful discussions and/or comments from Skee Houghton, Jim Randerson, Warren Cohen, Linda
646 Heath, and an anonymous reviewer. This work was funded by NASA NNH05ZDA001N, North
647 American Carbon Program. In addition, CAW was supported by the US National Science
648 Foundation under grant ATM-0910766.

649 **References**

650 Adler, R., et al. (2003), The Version-2 Global Precipitation Climatology Project (GPCP) monthly
651 precipitation analysis (1979-present), *Journal of Hydrometeorology*, *4*(6), 1147-1167.

652 Amiro, B. D., et al. (2000), Net primary productivity following forest fire for Canadian
653 ecoregions, *Canadian Journal of Forest Research-Revue Canadienne De Recherche*
654 *Forestiere*, *30*(6), 939−947.

655 Amiro, B. D., et al. (2011), Ecosystem carbon dioxide fluxes after disturbance in forests of North
656 America, *Journal of Geophysical Research*, *115*, G00K02.

657 Baker, D. F., et al. (2006), TransCom 3 inversion intercomparison: Impact of transport model
658 errors on the interannual variability of regional CO2 fluxes, 1988-2003, *Global*
659 *Biogeochemical Cycles*, *20*, GB1002, doi:1010.1029/2004GB002439.

660 Barford, C., et al. (2001), Factors controlling long-and short-term sequestration of atmospheric
661 CO2 in a mid-latitude forest, *Science*, *294*, 1688-1691.

662 Bechtold, W. A., and P. L. Patterson (2005), The enhanced Forest Inventory and Analysis
663 program—national sampling design and estimation procedures, SRS GTR-80, USDA Forest
664 Service, Southern Research Station, Asheville, North Carolina, USA.

665 Birdsey, R. A., and L. S. Heath (1995), Carbon changes in U.S. forests, in *Productivity of*
666 *America's Forests and Climate Change*, edited by L. A. Joyce, Fort Collins.

667 Bond-Lamberty, B., et al. (2004), Net primary production and net ecosystem production of a
668 boreal black spruce wildfire chronosequence, *Global Change Biology*, *10*, 473-487.

669 Bousquet, P., et al. (2000), Regional changes in carbon dioxide fluxes of land and oceans since
670 1980, *Science*, *290*(5495), 1342-1346.

671 Bradford, J. B., et al. (2008), Tree age, disturbance history, and carbon stocks and fluxes in
672 subalpine Rocky Mountain forests, *Global Change Biology*, *14*, 2882-2897.
673 Caspersen, J. P., et al. (2000), Contributions of land-use history to carbon accumulation in US
674 forests, *Science*, *290*(5494), 1148-1151.
675 Chapin III, F. S., et al. (2006), Reconciling carbon-cycle concepts, terminology, and methods,
676 *Ecosystems*, *9*, 1041-1050.
677 Cohen, W., et al. (2002), Characterizing 23 years (1972-95) of stand replacement disturbance in
678 western Oregon forests with Landsat imagery, *Ecosystems*(122-137).
679 Cole, C. T., et al. (2010), Rising concentrations of atmospheric CO_2 have increased growth in
680 natural stands of quaking aspen (*Populus tremuloides*), *Global Change Biology*, *16*, 2186-
681 2197.
682 EPA (2008), Inventory of U.S. Greenhouse Gas Emissons and Sinks: 1990-2006, United States
683 Environmental Protection Agency, edited, Washington, DC.
684 EPA (2010), Inventory of U.S. Greenhouse Gas Emissons and Sinks: 1990-2008, United States
685 Environmental Protection Agency, Washington, DC.
686 Fan, S., et al. (1998), A large terrestrial carbon sink in North America implied by atmospheric and
687 oceanic carbon dioxide data and models, *Science*, *282*, 442-446.
688 Gough, C. M., et al. (2007), The legacy of harvest and fire on ecosystem carbon storage in a
689 northern temperate forest, *Global Change Biology*, *13*, 1935-1949.
690 Goulden, M. L., et al. (2011), Patterns of NPP, GPP, respiration, and NEP during boreal forest
691 succession, *Global Change Biology*, *17*, 855-871.
692 Goward, S. N., et al. (2008), Forest disturbance and North American carbon flux, *EOS*
693 *Transactions, American Geophysical Union*, *89*(11), 105-106.

694 Gurney, K. R., et al. (2002), Towards robust regional estimates of CO2 sources and sinks using
695 atmospheric transport models, *Nature*, *415*(6872), 626-630.
696 Hansen, J., et al. (1999), GISS analysis of surface temperature change, *Journal of Geophysical*
697 *Research*, *104*, 30997-31022.
698 Harmon, M. E., and C. Hua (1991), Coarse woody debris dynamics in two old-growth
699 ecosystems, *BioScience*, *41*(9), 604-610.
700 Harmon, M. E., et al. (2004), Production, respiration, and overall carbon balance in an old-growth
701 Pseudotsuga-Tsuga forest ecosystem, *Ecosystems*, *7*, 498-512.
702 Hicke, J. A., et al. (2003), Postfire response of North American boreal forest net primary
703 productivity analyzed with satellite observations, *Global Change Biology*, *9*(8), 1145-1157.
704 Houghton, R. A. (1999), The annual net flux of carbon to the atmosphere from changes in land
705 use 1850-1990, *Tellus Series B-Chemical and Physical Meteorology*, *51*(2), 298-313.
706 Houghton, R. A., et al. (1999), The US carbon budget: Contributions from land-use change,
707 *Science*, *285*(5427), 574-578.
708 Houghton, R. A. (2003), Why are estimates of the terrestrial carbon balance so different?, *Global*
709 *Change Biology*, *9*(4), 500-509.
710 Hurtt, G. C., et al. (2002), Projecting the future of the US carbon sink, *Proceedings of the*
711 *National Academy of Sciences of the United States of America*, *99*(3), 1389-1394.
712 IPCC (2000), Intergovernmental Panel on Climate Change Good Practice Guidance and
713 Uncertainty Management in National Greenhouse Gas Inventories, Institute for Global
714 Environmental Strategies, Japan.
715 Ito, A., et al. (2008), Can we reconcile differences in estimates of carbon fluxes from land-use
716 change and forestry for the 1990s?, *Atmos. Chem. Phys.*, *8*, 3291-3310.

717 Janisch, J. E., et al. (2005), Decomposition of coarse woody debris originating by clearcutting of
718 an old-growth conifer forest, *Ecoscience*, *12*(2), 151-160.
719 Jokela, E. J., et al. (2004), Production dynamics of intensively managed loblolly pine stands in the
720 southern United States: a synthesis of seven long-term experiments, *Forest Ecology and*
721 *Management*, *192*, 117-130.
722 Joos, F., et al. (2002), Growth enhancement due to global atmospheric change as predicted by
723 terrestrial ecosystem models: consistent with US forest inventory data, *Global Change*
724 *Biology*, *8*, 299-303.
725 Kaminski, T., et al. (2001), Inverse modeling of atmospheric carbon dioxide fluxes, *Science*, *294*,
726 259.
727 King, A. W., et al. (2007), The First State of the Carbon Cycle Report (SOCCR): The North
728 American Carbon Budget and Implications for the Global Carbon Cycle, *NOAA, National*
729 *Climatic Data Center, Asheville, NC*.
730 Koerner, C. (2003), Slow in, rapid out - carbon flux studies and Kyoto targets, *Science*, *300*,
731 1242-1243.
732 Law, B. E., et al. (2002), Environmental controls over carbon dioxide and water vapor exchange
733 of terrestrial vegetation, *Agricultural and Forest Meteorology*, *113*(1-4), 97-120.
734 Law, B. E., et al. (2003), Changes in carbon storage and fluxes in a chronosequence of ponderosa
735 pine, *Global Change Biology*, *9*, 510-524.
736 Law, B. E., et al. (2004), Disturbance and climate effects on carbon stocks and fluxes across
737 Western Oregon USA, *Global Change Biology*, *10*, 1429-1444.

738 Leemans, R., and W. P. Cramer (1991), The IIASA Database for Mean Monthly Values of
739 Temperature, Preicipitation and Cloudiness of a Global Terrestrial Grid, RR-91-18, 62 pp,
740 IIASA, Laxenburg, Austria.
741 Litvak, M., et al. (2003), Effect of stand age on whole ecosystem CO2 exchange in the Canadian
742 boreal forest, *Journal of Geophysical Research*, *108*(D3), 8225.
743 Luyssaert, S., et al. (2010), The European carbon balance. Part 3: forests, *Global Change Biology*,
744 *16*, 1429-1450.
745 McGuire, A. D., et al. (2001), Carbon balance of the terrestrial biosphere in the twentieth century:
746 Analyses of CO2, climate and land use effects with four process-based ecosystem models,
747 *Global Biogeochemical Cycles*, *15*(1), 183-206.
748 McMahon, S. M., et al. (2010), Evidence for a recent increase in forest growth, *Proceedings of*
749 *the National Academy of Sciences*, *107*(8), 3611-3615.
750 Meigs, G. W., et al. (2007), Forest fire impacts on carbon uptake, storage, and emission: The role
751 of burn severity in the Eastern Cascades, Oregon, *Ecosystems*, *12*, 1246-1267.
752 Myneni, R. B., et al. (2001), A large carbon sink in the woody biomass of Northern forests,
753 *Proceedings of the National Academy of Sciences of the United States of America*, *98*(26),
754 14784-14789.
755 Nemani, R., et al. (2002), Recent trends in hydrologic balance have enhanced the terrestrial
756 carbon sink in the United States, *Geophysical Research Letters*, *29*(10).
757 Nightingale, J. M., et al. (2009), Temporally smoothed and gap-filled MODIS land products for
758 carbon modelling: application of the fPAR product, *International Journal of Remote Sensing*,
759 *30*, 1083-1090.

760 Noormets, A., et al. (2007), Age-related changes in forest carbon fluxes in a managed northern
761 Wisconsin landscape, *Ecosystems*, *10*, 187-203.
762 Odum, E. (1969), The strategy of ecosystem development, *Science*, *164*, 262-270.
763 Pacala, S. W., et al. (2001), Consistent land- and atmosphere-based US carbon sink estimates,
764 *Science*, *292*(5525), 2316-2320.
765 Pan, Y., et al. (2009), Separating effects of changes in atmospheric composition, climate and
766 land-use on carbon sequestration of U.S. Mid-Atlantic temperate forests, *Forest Ecology and*
767 *Management*, *259*, 151-164.
768 Pan, Y., et al. (2011), Age structure and disturbance legacy of North American forests,
769 *Biogeosciences*, *8*, 715-732.
770 Peters, W., et al. (2007), An atmospheric perspective on North American carbon dioxide
771 exchange: CarbonTracker, *Proceedings of the National Academy of Sciences of the United*
772 *States of America*, *104*, 18925-18930.
773 Potter, C. S., et al. (1993), Terrestrial Ecosystem Production - a Process Model-Based on Global
774 Satellite and Surface Data, *Global Biogeochemical Cycles*, *7*(4), 811-841.
775 Pregitzer, K. S., and E. S. Euskirchen (2004), Carbon cycling and storage in world forests: Biome
776 patterns related to forest age, *Global Change Biology*, *10*, 2052-2077.
777 Randerson, J. T., et al. (1996), Substrate limitations for heterotrophs: Implications for models that
778 estimate the seasonal cycle of atmospheric CO2, *Global Biogeochemical Cycles*, *10*(4), 585-
779 602.
780 Richter, D. D., et al. (1999), Rapid accumulation and turnover of soil carbon in a re-establishing
781 forest, *Nature*, *400*, 56-58.

782 Schimel, D., et al. (2000), Contribution of increasing CO2 and climate to carbon storage by
783 ecosystems in the United States, *Science*, *287*(5460), 2004-2006.
784 Schimel, D. S., et al. (2001), Recent patterns and mechanisms of carbon exchange by terrestrial
785 ecosystems, *Nature*, *414*(6860), 169-172.
786 Schwalm, C. R., et al. (2007), A method for deriving net primary productivity and component
787 respiratory fluxes from tower-based eddy covariance data: a case study using a 17-year data
788 record from a Douglas-fir chronosequence, *Global Change Biology*, *13*, 370-385.
789 Smith, J. E., and L. S. Heath (2001), Identifying influences on model uncertainty: An application
790 using a forest carbon budget model, *Environmental Management*, *27*(2), 253-267.
791 Smith, W. B., et al. (2009), Forest Resources of the United States, *Gen. Tech. Rep. WO-78,*
792 *Washington, DC: USDA, Forest Service, Washington Office.*, 336p.
793 Stephens, B. B., et al. (2007), Weak northern and strong tropical land carbon uptake from vertical
794 profiles of atmospheric CO2, *Science*, *316*, 1732-1735.
795 Tans, P. P., et al. (1990), Observational Constraints on the Global Atmospheric Co2 Budget,
796 *Science*, *247*(4949), 1431-1438.
797 Taylor, J. R. (1997), *An introduction to error analysis: The study of uncertainties in physical*
798 *measuremnts 2nd ed.*, 326 pp., University Science Books, Sausilito, California.
799 Thomas, R. Q., et al. (2009), Increased tree carbon storage in response to nitrogen deposition in
800 the US, *Nature-Geoscience*, *3*, 13-17.
801 Thompson, M. V., et al. (1996), Change in net primary production and heterotrophic respiration:
802 How much is necessary to sustain the terrestrial carbon sink?, *Global Biogeochemical Cycles*,
803 *10*(4), 711-726.

804 Thornton, P. E., et al. (2002), Modeling and measuring the effects of disturbance history and
805 climate on carbon and water budgets in evergreen needleleaf forests, *Agricultural and Forest*
806 *Meteorology*, *113*(1-4), 185-222.
807 Tinker, D. B., and D. H. Knight (2000), Coarse woody debris following fire and logging in
808 Wyoming lodgepole pine forests, *Ecosystems*, *3*, 472-483.
809 Turner, D. P., et al. (1995), A carbon budget for forests of the conterminous United States,
810 *Ecological Applications*, *5*(2), 421-436.
811 van der Werf, G. R., et al. (2010), Global fire emissions and the contribution of deforestation,
812 savanna, forest, agricultural, and peat fires (1997-2009). *Atmos. Chem. Phys.*, *10*, 11707-
813 11735.
814 Woodbury, P. B., et al. (2007), Carbon sequestration in the U.S. forest sector from 1990 to 2010,
815 *Forest Ecology and Management*, *241*, 14-27.
816 Yang, Z., et al. (2007), New constraints on Northern Hemisphere growing season net flux,
817 *Geophysical Research Letters*, *34*(12), L12807.
818 Zhang, Y.-C., et al. (2004), Calculation of radiative fluxes from the surface to top of atmosphere
819 based on ISCCP and other global data sets: Refinements of the radiative transfer model and
820 the input data, *Journal of Geophysical Research*, *109*, D19105, doi:
821 19110.11029/12003JD004457.
822 Zheng, D., et al. (2011), Carbon changes in conterminous US forests associated with growth and
823 major disturbances: 1992-2001, *Environ. Res. Lett.*, *6*, 014012.
824 Zhou, L., et al. (2003), Relation between interannual variations in satellite measures of northern
825 forest greenness and climate between 1982 and 1999, *Journal of Geophysical Research-*
826 *Atmospheres*, *108*(D1).

827 Zhu, Z., and D. L. Evans (1994), US forest types and predicted percent forest cover from AVHRR
828 data, *Photogrammetric Engineering and Remote Sensing*, *60*, 525-531.

829
830

Figure Captions.

Figure 1. Schematic diagram illustrating stock and flux (italicized) relationships between the forest sector and atmosphere. The entire forest sector net flux (sink) as defined by the stock-change approach is: Net Flux = $\Delta\ C_{stocks} + \Delta\ C_{wood\ products}$. Alternatively, using our model driven estimates of *NEP* it is: Net Flux = *NEP – Wood Products Emissions – Fire*.

Figure 2. Conterminous U.S. distribution of forest type groups shown with thick state boundaries that trace regions from the Resource Planning Act Assessment by the US Forest Service. Colors differentiate FIA forest type groups. The rectangles represent areas where gridded climate and phenology were used in the simulation of fluxes and stocks for each forest type within each rectangle.

Figure 3. Characteristic trajectories of aboveground live wood biomass regrowth and associated carbon sources / sinks (expressed as net ecosystem productivity, *NEP*) following a stand-replacing disturbance in high productivity Douglas-fir stands of the Pacific Northwest. Results are from the CASA model fit to regrow stocks consistent with 25 independent samples from the forest inventory data (red circles). Net releases in the year following disturbance are as low as -3000 g C m^{-2} a^{-1} (see Auxiliary Material 2, Figure A2.2) rising to above -500 g C m^{-2} a^{-1} in the second year of regrowth.

Figure 4a,b. Map of average net ecosystem productivity (top, a) and uncertainty expressed as one standard deviation (bottom, b) (*NEP* in g C m^{-2} a^{-1}) for forests of the conterminous US.

852 Table 1. Regional distribution of forest area, live biomass (Live *B*), ratio of *EPA* [2008] to this
853 study's forest area (f_{EPA08} Area), ratio of *EPA* [2008] to this study's live biomass (f_{EPA08} Live *B*),
854 net ecosystem productivity (*NEP*), fraction of forest that is less than 25 years old (<25y), less than
855 5 years old (<5y).

Region	Area	Live *B*	f_{EPA08}	f_{EPA08}	*NEP*	<25y	<5y
--	[10^9 m^2]	[Tg C]	Area [--]	Live *B* [--]	[Tg C a^{-1}]	[%]	[%]
NE	339	3,253	1.11	1.01	32±5.5	10	2
NLS	212	1,236	0.99	1.11	12±1.3	16	3
SE	355	2,621	1.00	0.94	30±3.5	39	8
SC	384	3,220	1.27	1.00	40±4.2	37	8
RMN	192	1,189	0.98	1.10	7±1.8	21	5
RMS	493	1,815	0.81	0.97	11±5.5	1	0
PSW	127	1,522	1.06	0.95	13±2.8	11	2
PNW	202	2,162	1.05	1.13	18±3.0	19	4
Total/Mean	2,303	17,017	1.03	1.08	164±27.7	17	4

856
857

858 Table 2. Changes in carbon stocks [Tg C a^{-1}] in the year 2005 reported in different studies.
859 Italicized values are inferred from mass balance.

	This Study	*EPA* [2008]
ΔTotal Soil C	3	9
ΔLitter C	1	15
ΔCoarse Woody Debris (CWD)	4	16
ΔCWD Below	0	--
ΔLive C	39	133
Total Stock Change	47	173
Removals[g]	117	*162*
Harvest[a]	*107*	132
Wildfire Emissions[b]	10	30
NEP[c]	164	*335*
Wood Products Emissions[d]	102	102
Wood Products Storage[e]	*5*	30
Forest Sector - Atmosphere Exchange[f]	52	203

860 [a]this study inferred as: Harvest = Removals – Wildfire Emissions;
861 [b]this study estimated wildfire emissions from the Global Fire Emissions Database v3 (GFED3)
862 [*van der Werf et al.*, 2010];
863 [c]for the purposes of this table calculated as:
864 *NEP* = ΔTotal Soil C + ΔLitter C + ΔCWD + ΔCWD Below + ΔLive C + Removals; values
865 differ from those in Table 1 due to differences in the method of aggregation and associated
866 averaging of terms;
867 [d]this study adopted values reported in *EPA* [2008];
868 [e]this study calculated as:
869 Wood Products Storage = Removals – Wood Products Emissions – Wildfire Emissions;
870 [f]this study calculated as:
871 Forest Sector-Atmosphere Exchange = *NEP* – Wood Products Emissions – Wildfire Emissions;
872 [g]for *EPA* [2008] calculated as: Removals = Wildfire Emissions + Harvest.

Table 3. Forest carbon *NEP* and stock change for the conterminous US [Tg C a^{-1}] from this and a sample of previously published estimates. Estimates are classified according to approach: age structure–C accumulation (*A&A*), stock change (ΔC_{stocks}=*NBP*), or process model (*P*), where *P* is a process model ensemble result that accounts for CO_2 and climate effects [*Schimel et al.*, 2000], and *Pacala et al.* [2001] combines approaches for an overall estimate and range. Low and High refers to 1 standard deviation about the mean estimate.

Source	Approach	Mean *NEP*	Low	High	ΔC_{stocks}	*Harvest*	*Fire*
Schimel et al. [2000][a]	*P*	80					
This Study[b]	*A&A*	164	136	192	47	107	10
Houghton et al. [1999][c]	*A&A*	182			10	92	80
Turner [1995][e]	*A&A*	203			79	124	0
Houghton [2003][d]	*A&A*	207			35	92	80
Woodbury et al. [2007][f]	ΔC_{stocks}	270	256	293	108	132	30
EPA [2008][g]	ΔC_{stocks}	335			173	132	30
Birdsey & Heath [1995][h]	ΔC_{stocks}	368			211	127	30
Hurtt et al. [2002][i]	*A&A*	372	282	442	230	92	50
Pacala et al. [2001][j]	synthesis	392	312	472	220	92	80
King et al. [2007][k]	ΔC_{stocks}	411	383	439	236	145	30

a) for 1980-1993
b) for 2005, C stock change = *NEP – Harvest – Fire*, see Table 2, our total removals are 117 Tg C a^{-1} that includes fire and harvest, assume fire at 10 Tg C a^{-1} (see GFED3 of *van der Werf et al.*[2010] and *Zheng et al.* [2011])
c) 1980s
d) for 1990's, harvest and fire from *Houghton et al*. [1999]
e) for ~1990,
f) for 2005
g) for 2005
h) for 1992
i) for 1980s
j) for 1980's
k) for 1980s

Figure 1. Schematic diagram illustrating stock and flux (italicized) relationships between the forest sector and atmosphere. The entire forest sector net flux (sink) as defined by the stock-change approach is: Net Flux = $\Delta C_{stocks} + \Delta C_{wood\ products}$. Alternatively, using our model driven estimates of *NEP* it is: Net Flux = *NEP – Wood Products Emissions – Fire Emissions*.

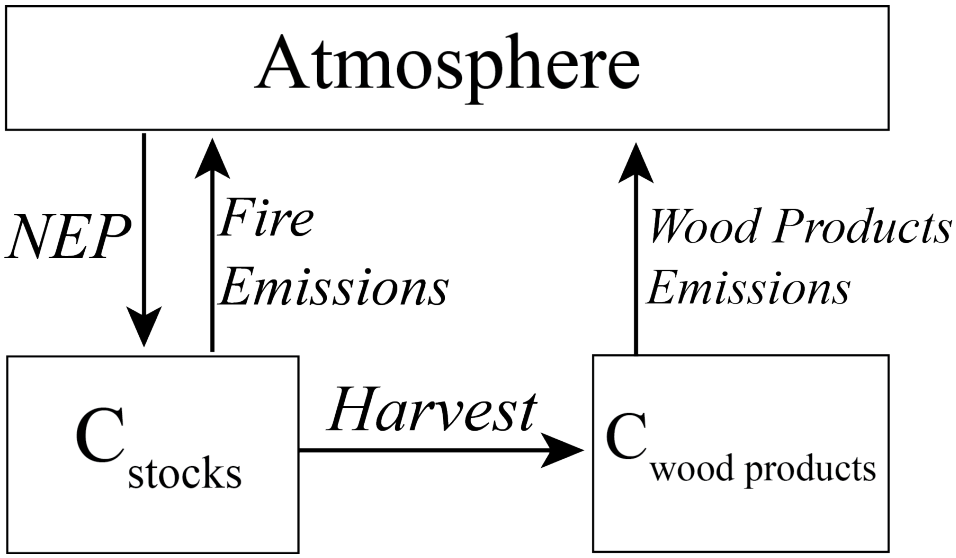

Figure 2. Conterminous U.S. Forest Type Groups shown with thick state boundaries that trace regions from the Resource Planning Act Assessment by the US Forest Service. Colors differentiate FIA forest type groups. The rectangles represent areas where gridded climate and phenology were used in the simulation of fluxes and stocks for each forest type within each rectangle.

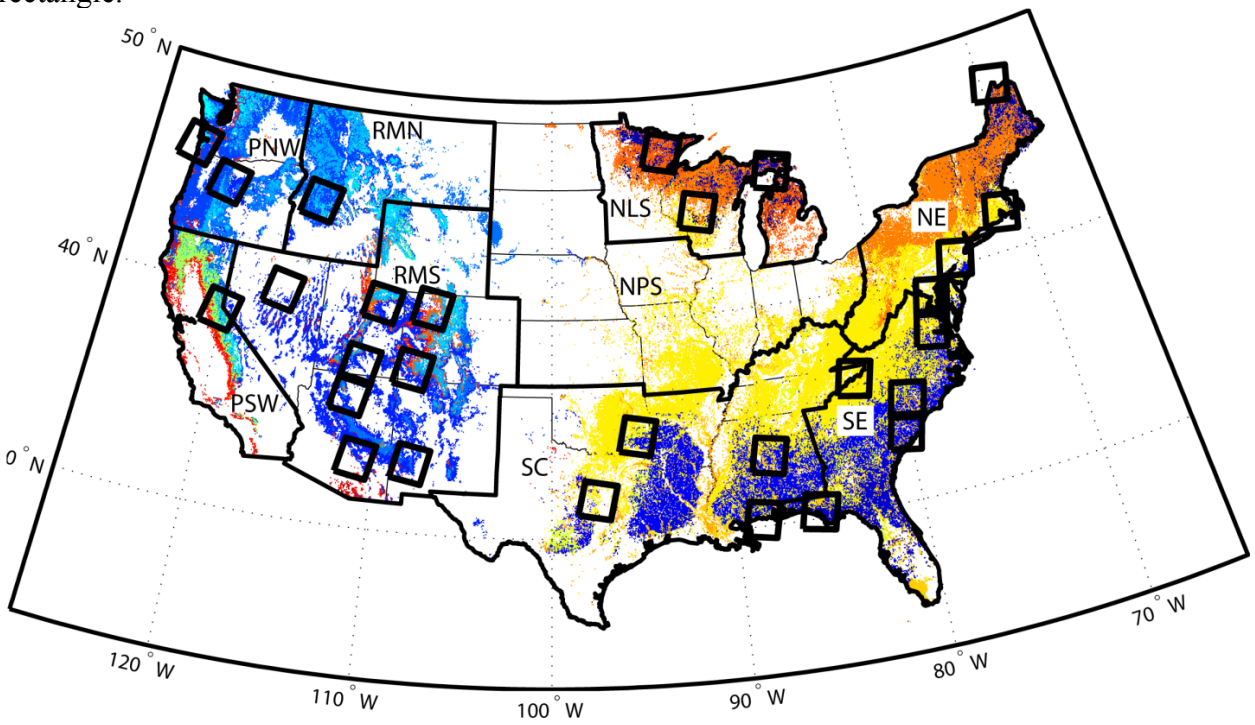

Figure 3. Characteristic trajectories of aboveground live wood biomass regrowth and associated carbon sources / sinks (expressed as net ecosystem productivity, *NEP*) following a stand-replacing disturbance in high productivity Douglas-fir stands of the Pacific Northwest. Results are from the CASA model fit to regrow stocks consistent with 25 independent samples from the forest inventory data (red circles). Net releases in the year following disturbance are as low as -3000 g C m^{-2} a^{-1} (see Auxiliary Material 2, Figure A2.2) rising to above -500 g C m^{-2} a^{-1} in the second year of regrowth.

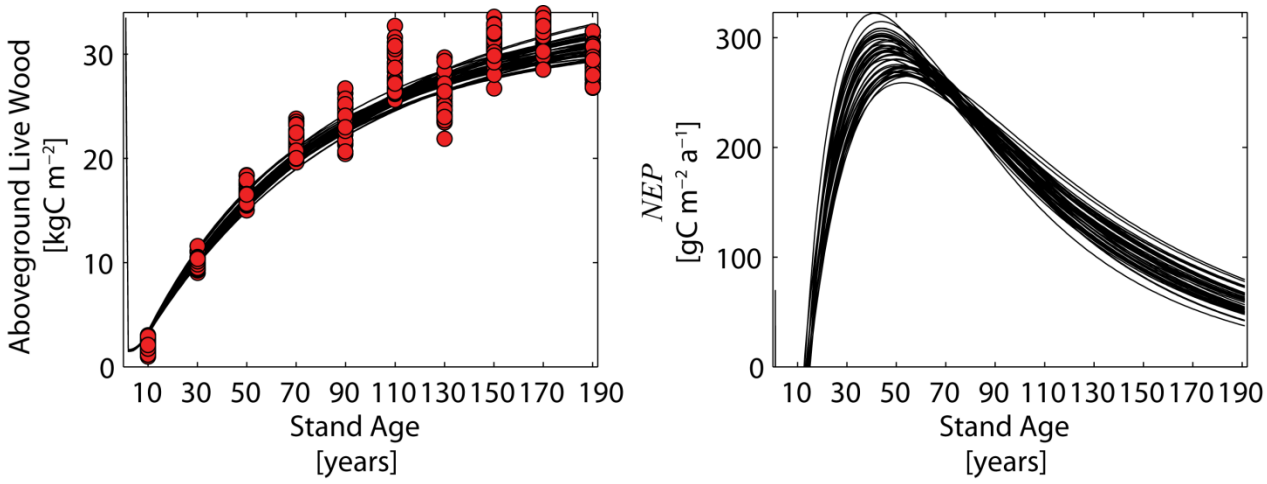

Figure 4a,b. Map of average net ecosystem productivity (top, a) and uncertainty expressed as one standard deviation (bottom, b) (*NEP* in g C m^{-2} a^{-1}) for forests of the conterminous US.